Self-consistent electronic spectrum of trigonal Te. Pressure dependence of energy spectrum

H. Isomäki
Department of General Sciences, Helsinki University of Technology, SF-02150 Espoo 15, Finland

J. von Boehm*
NORDITA, DK-2100 Copenhagen Ø, Denmark

P. Krusius† and T. Stubb
Electron Physics Laboratory, Helsinki University of Technology and Semiconductor Laboratory, Technical Research Centre of Finland, SF-02150 Espoo 15, Finland

(Received 5 December 1979)

The behavior of the energy bands and core levels of trigonal Te under hydrostatic pressure up to 38 kbar is calculated within the X_α scheme for $\alpha=\frac{2}{3}$ and 1 using the fully self-consistent symmetrized orthogonalized-plane-wave method. The results are compared with those of the self-consistent pseudopotential method and experiments. The optical gap is direct and remains at H at all pressures. The margins to the next valence-band maximum and conduction-band minimum increase with increasing pressure. At room temperature the optical gap is estimated to be less than kT at $\approx$40 kbar. The valence density of states shows a close resemblance to the x-ray-photoemission spectra. The core levels are found to be insensitive to pressure. The relativistically corrected $\alpha=1$ core levels are more negative than the experimental ones (except $3s$). This allows positive relaxation corrections.

I. INTRODUCTION

Crystalline Te and Se are continually subject to active interest.[1] This is due to the highly anisotropic one-dimension-like crystal structure which causes many unexpected effects in their physical behavior. Both semiconductors crystallize into parallel helical chains arranged in a hexagonal array. Each atom has two nearest neighbors within the same chain. Three adjacent atoms of the same chain belong to one primitive unit cell. The space group of the crystal with a right-hand screw axis is D_3^4. The bonds between adjacent atoms within the chains are strong (and covalent), whereas the bonding between the chains is much weaker but by no means negligible. In fact many physical properties would be impossible to understand without taking the interchain interactions properly into account.

Te is experimentally a well-controlled material. This fact is expressed by the existence of high-quality single crystals and quantitatively similar results from independent experiments (for reviews see Refs. 2–4). Because of these stringent experimental tests and also the anisotropy, Te has been an arduous challenge for band theorists. In the past, several attempts have been made to calculate the electronic energy-band structure of Te.[5–20] However, the resulting bands have been only partially successful in interpreting experimental data. The reason for this has turned out to be various approximations involved in the calculations and the missing self-consistency. The use of a general effective potential along with a full self-consistency is of crucial importance as is successfully demonstrated in the recent self-consistent pseudopotential (SCPP) calculations for Te by Starkloff and Joannopoulos.[21,22] But even in their approach the pseudopotential contains a function with two adjustable parameters.

In this paper we present energy-band results for Te from our fully parameter free, well-converged, self-consistent symmetrized orthogonalized plane wave (SCSOPW) calculations.[23] In our approach both valence and core electrons experience the same general (i.e., non-muffin-tin) effective potential and both valence and core states are treated in the self-consistent way. This also allows us to present the self-consistent core-level spectra. The same SCSOPW method has been earlier applied successfully to trigonal Se[24,25] and the recent photoluminescence measurements by Moreth[26] support the

SCSOPW assignment of the nonrelativistic optical gap to the $M \rightarrow H$ transition.

Recently the behavior of Se and Te under hydrostatic pressure has aroused much interest. Controversies have appeared in the interpretation of the strong enhancement and anisotropy anomaly in the reflectivity spectra.[27–29] Other controversies have been associated with the location of the optical gap under pressure[30] as well as the driving mechanism and the exact pressure of the transition of Te from the insulating phase to the metallic.[31–38] In order to study these questions we have also calculated the behavior of the band structure of Te under hydrostatic pressure up to 38 kbar, where this transition is believed to occur.

The format of the present paper is as follows. In Sec. II we present briefly the formalism, including comments on the X_α theory we used and a description of the SCSOPW method. Section III contains our results and a discussion and Sec. IV conclusions. In the next paper[39] we present the second part of our study on Te comprising the charge and momentum densities and the Compton profiles.

II. FORMALISM

In the X_α theory the exchange and correlation effects are incorporated via a term proportional to $\rho^{1/3}$ (ρ is the electron density in the effective one-electron Schrödinger equation). Depending on the way this equation is derived, one can get two values for the constant α multiplying the exchange-correlation term: $\alpha = \frac{2}{3}$ (Dirac,[40] Gáspár,[41] Kohn and Sham[42]) or $\alpha = 1$ (Slater[43]). The former value seems to be better founded theoretically, whereas the latter seems to give energies which agree better with experiments. We do not want to go into deeper discussion about their relative merits here, but present the results for both values. In this way one also gets some idea of what the intermediate values ($\frac{2}{3} < \alpha < 1$) would give.

Strictly speaking, Koopman's theorem is not valid in the X_α theory. For this reason all excitation energies should be calculated using a transition state[44] (a self-consistent calculation with a half electron transferred from the initial state to the final state). This method, also including effects of the relaxation, is clearly important when calculating excitation energies in small systems like atoms, molecules, and clusters. However, as argued by Slater,[44] the transfer of a half electron from an initial extended Bloch state to a final Bloch state cannot result in a transition-state energy difference deviating from the corresponding X_α energy-band difference. In other words, the relaxation effects are here negligible. This justifies the direct use of energy bands in the X_α theory. (The transitions associated with the localized core states are still subject to large relaxation effects, of course.) The authors of Ref. 29 argue that the transition state should be taken into account by giving fractional occupation for the initial and final band triplets associated with the transition. However, in light of the considerations above, this does not seem to be justified because it would mean a transfer of a fraction of the roughly 10^{23} electrons instead of a half electron. Also, the justification of using $\alpha = 1$ in approximating a transition state with $\alpha \approx 0.7$ seems to be questionable in this connection.[22]

The SCSOPW method used in our calculations is described in detail in Ref. 24, and only a brief description will be given here. The valence states are spanned as a linear combination of symmetry adapted OPW's (SOPW) orthogonal to the localized core states. The iteration proceeds as follows. First, using an educated guess for the crystal potential (e.g., a linear combination of atomic potentials), one calculates the valence states and from these the valence electron density.[45] Freezing this density one iterates new core states using Herman-Skillman[46]-like programs until self-consistency is achieved. New valence states are then calculated from the effective Schrödinger equation where the (general nonmuffin-tin) potential energy is formed from the previous valence and new core-electron densities. From these new valence states one calculates the corresponding electron density, which is again freezed during the evaluation of new core states. The calculation continues in this way until the valence electron density as well as the energy bands have converged within a certain accuracy.

Because of computational limitations, the valence states were calculated only at the high-symmetry points Γ, A, H, K, H', and K' (H' and K' related to H and K by time-reversal symmetry) of the first Brillouin zone (BZ) (see Fig. 2 below). The valence electron density was evaluated as a weighted sum over these points. Fortunately, the results for Te depend very little on the representative $\vec{k}$ set. For example the self-consistent valence eigenvalues at Γ calculated on one hand with the set $\{\Gamma\}$ and on the other hand with the set $\{\Gamma, A, K, H, K', H'\}$ (150 SOPW's per symmetry point) differ by less than 0.1 eV. In addition to the convergence with respect to the number of $\vec{k}$ vectors we have also the one with respect to the number of SOPW's per $\vec{k}$ point. Figure 1 shows this convergence for the valence eigenvalues and the conduction-band edge at Γ calculated self-consistently using the set $\{\Gamma, A, K, H, K', H'\}$. The convergence is very good. The eigenvalues for 200 and 235 SOPW's differ by less than 0.04 eV. In the final calculations the set $\{\Gamma, A, K, H, K', H'\}$ and 235 SOPW's per $\vec{k}$ point were used.

After the self-consistent results were obtained the valence density of states (VDOS) at zero pressure was calculated as follows. The final SCSOPW poten-

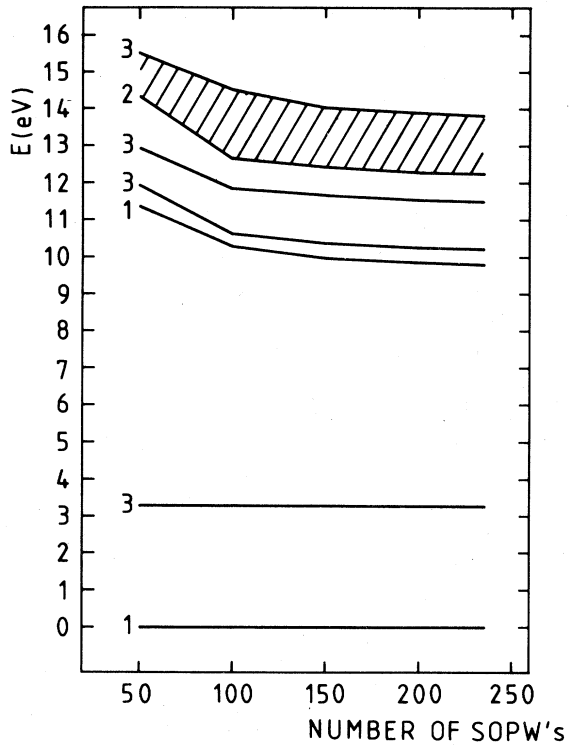

FIG. 1. The convergence of the energies at Γ with respect to the number of SOPW's. All energies are scaled with respect to the lowest energy. The curves are based on self-consistent calculations with the set {Γ, *A*, *K*, *H*, *K'*, *H'*} and SOPW numbers 50, 100, 150, 200, and 235 per symmetry point ($\alpha=1$). The integers at the curves are labels for the irreducible representations.

tial was used in calculating the valence energy eigenvalues in a regular grid consisting of 10 points in 8 equidistantly spaced planes perpendicular to the k_z axis in the irreducible segment of BZ (corresponding to 64 symmetry-independent $\vec{k}$ points, see Fig. 4 below). The same mesh is also used in calculating the momentum-space quantities of Te.[39] For $\alpha=\frac{2}{3}$ and 1 we used 159 and 145 OPW's per $\vec{k}$ point, respectively. The VDOS was then calculated using a straightforward histogram method.

III. RESULTS AND DISCUSSION

The SCSOPW energy bands of Te were calculated at the pressures 0, 8, and 38 kbar using the α values $\frac{2}{3}$ and 1 (for lattice constants see Table I[35,47,48]). The bands associated with these two α values at zero pressure as well as their changes under pressure are qualitatively very similar. We have plotted the $\alpha=1$ bands along the main symmetry lines at the pressures 0 and 38 kbar in Fig. 2 where the tendency of the bands to broaden with increasing pressure is clearly seen. In Fig. 3 we have plotted the $\alpha=\frac{2}{3}$ bands at zero pressure and indicated the main differences with respect to the corresponding $\alpha=1$ bands. The key quantities of the SCSOPW and SCPP bands are given in Table I.

We consider first the zero-pressure situation. It is generally known that the increase of α tends to narrow bands and increase gaps. One immediately notices from Fig. 3 and Table I that this tendency is present also in our SCSOPW bands. (Notice though the larger optical gaps at Γ and *K* in the case of $\alpha=\frac{2}{3}$.) The largest differences caused by the use of different α values occur at the upper part of the lowest (*s*-bonding[19]) valence-band triplet (VB_1), in the direct optical gap at *K* and in the gap between the lower and upper conduction-band triplets (CB_1 and CB_2, respectively). The decrease of α from 1 to $\frac{2}{3}$ increases the width of CB_1 by $\approx$0.3–0.5 eV. However, the major effect is to shift CB_2 towards CB_1 by $\approx$1–2 eV. This causes the direct gap between CB_1 and CB_2 at *L* of about 0.6 eV to close (overlap $\approx$1.3 eV). The SCSOPW and SCPP bands ($\alpha=1$) are relatively similar in the neighborhood of the optical gap (see Fig. 2 and Refs. 21 and 22). The optical-gap region of the SCPP bands is $\approx$0.2 eV broader than the one of the SCSOPW bands (except at *K* and *L*) (Table I). We will discuss the questions related to the optical gap more thoroughly below. The principal differences between the SCSOPW and SCPP bands follow. The SCSOPW VB_1 is $\approx$0.8 eV broader than the SCPP VB_1. The total width of the middle (*p*-bonding[19]) plus the uppermost (*p*-nonbonding[19]) SCSOPW valence-band triplets (VB_2 and VB_3, respectively) is $\approx$0.4 eV larger than the corresponding SCPP value (see Table I).

Next we will relate our SCSOPW bands with experiments. The main features of the VDOS are usually reflected in the x-ray-photoemission (XPS) spectrum. However, it should be kept in mind that a direct comparison involves several assumptions. The matrix elements (i.e., transition probabilities) from the valence states to the final states at $\approx$1000-eV higher energies are assumed constant. All effects associated with the surface (i.e., a possible direct surface contribution, the effect during the transport of the electrons to the surface and the escape of the electrons away from the surface) are neglected. Also the resolution of $\approx$0.5 eV of the XPS measurement rounds off the experimental curves. The XPS results of Pollak *et al.*[49] for Te show the VB_3, VB_2, and broad VB_1 maxima at the energies of about −2, −4.5, and −12 eV, respectively. Using far-ultraviolet and x-ray photoemission Shevchik *et al.*[50] found that the VB_2 maximum in fact consisted of two maxima. The more recent XPS measurement by Schlüter *et al.*[51] also shows two maxima at VB_1. Our SCSOPW VDOS for

TABLE I. Key quantities of the self-consistent band structures at different hydrostatic pressures. The energies at M and L are calculated in the final SCSOPW potential with 235 SOPW's. All energies are given in eV. The SCSOPW lattice constants at zero pressure are slightly corrected to correspond to the zero temperature situation. VB_1, VB_2, VB_3, CB_1, and CB_2 denote the three valence-band and two conduction-band triplets with increasing energy. Γ, A, H, K, L, and M denote symmetry points of BZ (see Fig. 2). VB and CB denote valence band and conduction band, respectively. The group-theoretical labels in parentheses denote the next maxima or minima.

Property	SCSOPW $\alpha=\frac{2}{3}$ 0 kbar	SCSOPW $\alpha=1$ 0 kbar	SCPP $\alpha=1$ 0 kbar	SCSOPW $\alpha=\frac{2}{3}$ 8 kbar	SCSOPW $\alpha=1$ 8 kbar	SCPP $\alpha=1$ 8 kbar	SCSOPW $\alpha=\frac{2}{3}$ 38 kbar	SCSOPW $\alpha=1$ 38 kbar	SCPP $\alpha=1$ 38 kbar
a (Å)	4.4572[a]	4.4572[a]	4.457[a]	4.378[b]	4.378[b]	4.378[b]	4.241[b]	4.241[b]	4.241[b]
c (Å)	5.929[a]	5.929[a]	5.929[a]	5.948[b]	5.948[b]	5.948[b]	5.972[b]	5.972[b]	5.972[b]
u (a)	0.2633[a]	0.2633[a]	0.263[a]	0.2670[c]	0.2670[c]	0.267[c]	0.2705[c]	0.2705[c]	0.2705[c]
Width of VB_1	6.40	5.56	4.79	6.64	5.78	4.98	7.18	6.29	5.33
Gap between VB_1 and VB_2	0.64	2.05	3.03	0.38	1.79	2.84	−0.20	1.24	2.49
Width of VB_2	3.27	2.66	2.52	3.54	2.89	2.84	4.05	3.37	3.27
Overlap of VB_2 and VB_3	0.88	0.39	0.52	1.16	0.63	0.85	1.50	1.09	1.17
Width of VB_3	3.66	3.05	2.89	3.90	3.29	3.07	4.16	3.69	3.32
Width of VB_2 plus VB_3	6.04	5.32	4.89	6.28	5.55	5.06	6.71	5.97	5.42
Direct gap at Γ	1.69	1.59	1.74	1.74	1.62	1.77	1.81	1.69	1.86
A	1.32	1.38	1.52	1.21	1.28	1.44	1.08	1.15	1.32
H	0.04	0.24	0.44	−0.08	0.12	0.33	−0.25	−0.07	0.13
K	5.60	4.96	4.81	5.92	5.25	5.07	6.50	5.79	5.56
L	1.73	1.81	1.76	1.67	1.74	1.72	1.63	1.69	1.67
M	0.74	0.87	1.08	0.66	0.80	1.02	0.55	0.69	0.94
Indirect gap $M_2 \rightarrow H_1$	0.26	0.34	0.59	0.24	0.30	0.54	0.23	0.26	0.49
Location of VB maxima	H_3, (M_2)	H_3, (M_2)	H_3, (M_2)	H_3, (M_2)	H_3, (M_2)	H_3, (M_2)	H_3, (M_2)	H_3, (M_2)	H_3, (M_2)
ΔE between VB maxima $H_3 - M_2$	0.23	0.10	0.15	0.31	0.18	0.21	0.48	0.32	0.36
Location of CB minima	H_1, (A_1,M_1)	H_1, (A_1,M_1)	H_1, (A_1,M_1)	H_1, (A_1,M_1)	H_1, (A_1,M_1)	H_1, (A_1,M_1)	H_1, (A_1,M_1)	H_1, (A_1,M_1)	H_1, (M_1,A_1)
ΔE between CB minima $A_1 - H_1$, ($M_1 - H_1$)	0.14, (0.48)	0.23, (0.53)	0.30	0.19, (0.42)	0.27, (0.50)	0.37, (0.48)	0.31, (0.32)	0.38, (0.44)	(0.45)
Width of CB_1	3.70	3.20	2.87	3.86	3.36	3.08	4.15	3.67	3.56
Gap between CB_1 and CB_2	−1.25	0.55	0.55	−1.47	0.30	0.27	−1.84	−0.13	−0.20
Width of CB_2	5.90	5.27		6.17	5.53		6.52	5.89	

[a]Reference 47.

[b]Reference 35.

[c]Reference 48.

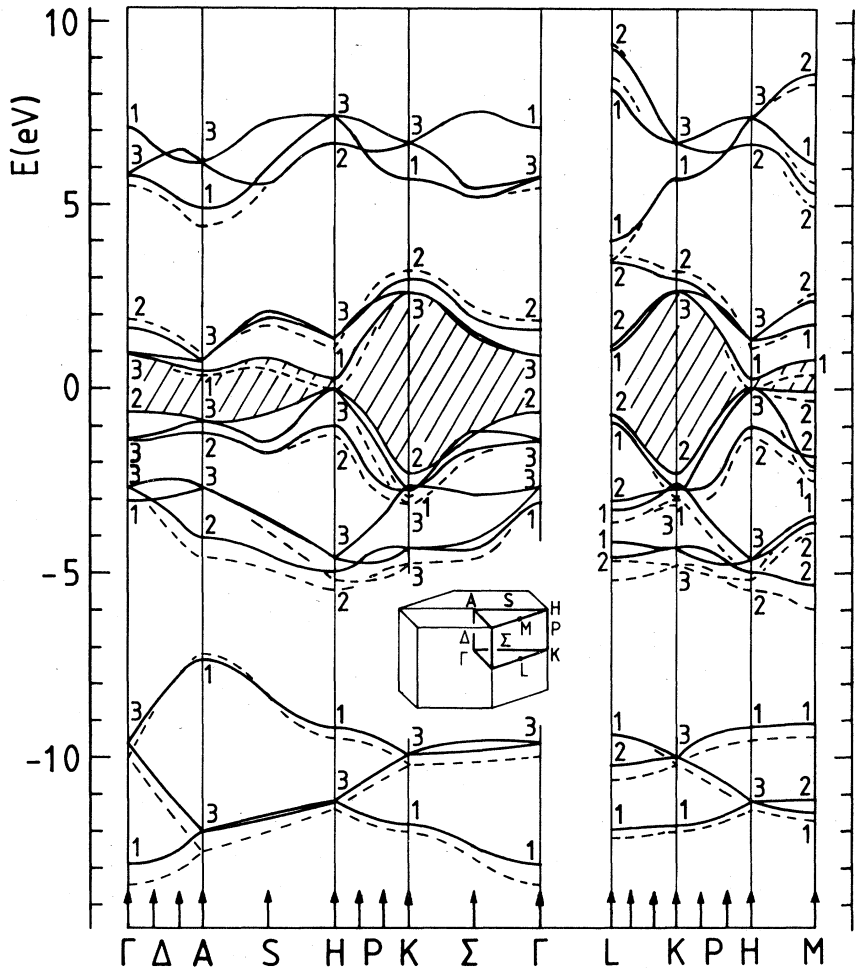

FIG. 2. The SCSOPW $\alpha = 1$ energy bands of Te. Full lines and broken lines represent 0- and 38-kbar bands, respectively. The set {Γ, *A*, *K*, *H*, *K'*, *H'*} and 235 SOPW's per symmetry point were used. The bands are based on the SCSOPW eigenvalues calculated using the SCSOPW potential at the $\vec{k}$ points indicated by vertical arrows as well as on the compatibility relations. The valence-band maxima at *H* are placed to 0 eV. For lattice constants see Table I. The integers 1, 2, and 3 label the irreducible representations. BZ with symmetry labels is also inserted.

both α values at zero pressure are displayed with this XPS result in Fig. 4. The arrows indicate the peak positions of the SCPP VDOS. Our $\alpha = 1$ SCSOPW VDOS agrees well with the XPS result with the minor exception that the upper VDOS peak at VB_1 lies $\approx$0.5 eV higher than the corresponding XPS maximum. Because of the broader energy bands the three middle peaks of the $\alpha = \frac{2}{3}$ SCSOPW VDOS are shifted towards the VB_1-VB_2 gap which makes the agreement with the XPS result worse than for $\alpha = 1$. The agreement between the $\alpha = 1$ SCSOPW and SCPP VDOS is quantitatively very close (i.e., within the accuracy $\approx$0.3 eV of our histogram).

Wautelet and Laude[52] estimate from double-beam photoemission the distances from the valence-band (VB) maximum to the CB_1 maximum and the CB_2 minimum to be 2.5 and 4.7 eV, respectively. The corresponding $\alpha = 1$ SCSOPW and SCPP distances are both $\approx$3.5 and 4 eV. (As discussed earlier the SCSOPW $\alpha = \frac{2}{3}$ CB_1-CB_2 gap closes.)

When the hydrostatic pressure is applied the energy bands should broaden and the gaps tend to close. The SCSOPW and SCPP band structures follow these general trends (Table I and Fig. 2). However, the similarity is even closer. For example, the exceptional increasing behavior of the direct gap at symmetry points Γ and *K* with increasing pressure is present in all band structures.

In Table II[21, 22, 30, 36, 53–57] we summarize both experimental and theoretical coefficients describing

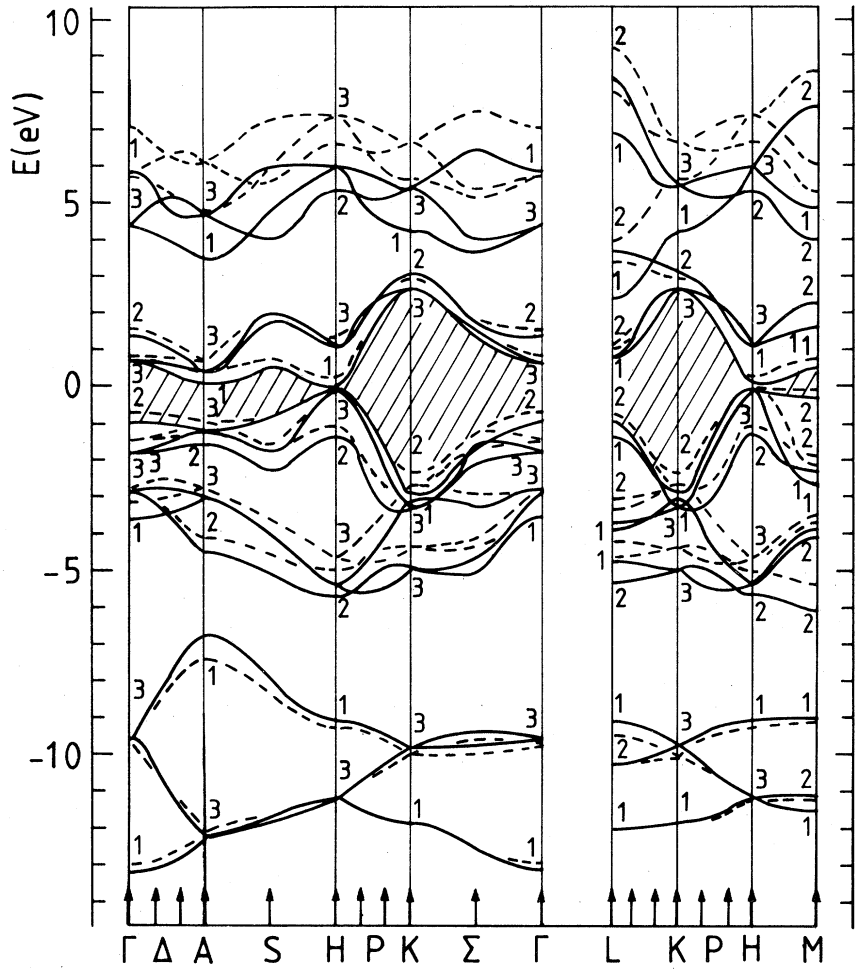

FIG. 3. The SCSOPW $\alpha=\frac{2}{3}$ energy bands of Te. Full lines and broken lines represent $\alpha=\frac{2}{3}$ and 1 bands at zero pressure, respectively. For further information see the caption of Fig. 2.

the dependence of the optical gap E_g on the hydrostatic pressure P. We have used the exponential function

$$E_g = Ae^{-\beta P} - B \tag{1}$$

as a fit to the SCSOPW results and the experimental data of Blum and Deaton.[36] The coefficients A, β, and B in the latter case are obtained using the information that $E_g(0)=0.33$ eV, $(\partial E_g/\partial P)_{p=0}=-0.017$ eV/kbar, and $E_g(43\text{ kbar})=0$. The SCSOPW coefficients result from the fit to the results at 0, 8, and 38 kbar (Table I). Anzin *et al.*[57] have also used Eq. (1) as their gap function. Other authors use a linear or parabolic function. (The values of A, β, and B given in parentheses for the gap function of Pine *et al.*[30] are from Ref. 58.) The information of coefficients of the linear and parabolic functions is implicitly included in the last three columns of Table II where the values and derivatives of the gap functions at zero pressure are given. It is obvious that the slopes $(\partial E_g/\partial P)_{P=0}$ of the transport experiments tend to be less negative than those of the optical experiments. The theoretical SCPP and SCSOPW slope values fall between the experimental ones. Of the experimental values the laser-emission value of −0.02 eV/kbar by Pine *et al.*[30] may be considered to be most reliable. The SCSOPW $\alpha=1$ value −0.01866 eV/kbar is in good agreement with this value. The good agreement applies even to the corresponding curvatures: The experimental and theoretical second derivatives at zero pressure are 0.001 04 and 0.000 983 8 eV/kbar^2, respectively. The SCSOPW $\alpha=\frac{2}{3}$ values show a slightly less good agreement with this experiment. The transmission and photoconductivity gap functions by Anzin *et al.*[57] are in a close agreement with the laser-emission gap function. The SCPP slope value agrees best with the slopes of the earlier transport measurements.[36,53,55,56] However, the SCPP second derivative is smaller than any of the experimental ones and less than 40% of the SCSOPW $\alpha=1$ value.

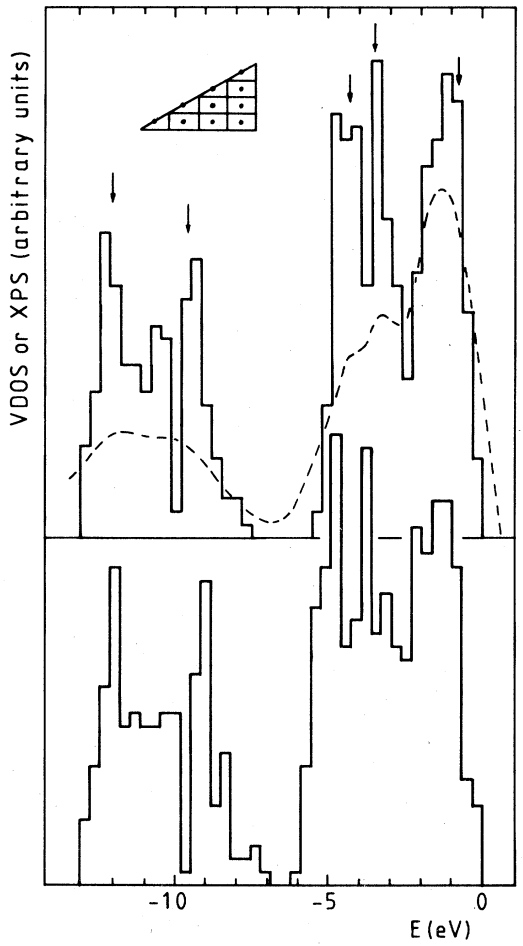

FIG. 4. The SCSOPW VDOS of Te. The upper and lower histograms are the SCSOPW $\alpha = 1$ and $\frac{2}{3}$ VDOS, respectively, given in the same arbitrary units. The dashed line is the XPS result of Schlüter *et al.* (Ref. 51). In the upper left-hand corner the grid used in the calculations of the histograms is indicated. Grid consists of ten points in each of the planes $k_z = -7b_3/16, -5b_3/16, \ldots, 7b_3/16$ ($b_3 = 2\pi/c$) inside the irreducible segment of BZ.

It is generally believed that the photon absorption for light polarized $\perp c$ is due to direct transitions at the corner point H. However, there has been a controversy whether the absorption for light polarized $\| c$ is due to indirect (allowed) transitions[59] or direct forbidden transitions at H.[60,61] According to Kosichkin,[58] the latter alternative is to be preferred because, contrary to the measurements of Neuringer[54] (see Table II), the slopes of the gap functions for both light polarizations measured by Anzin *et al.*[57] do not differ significantly and because the magnetic absorption measurements give the same gap values.[60,61] Provided that the optical-absorption energies for both light polarizations are the same both the SCSOPW

TABLE II. The dependences of the minimum optical gaps E_g on the hydrostatic pressure P. Lin., Par., and Exp. denote linear, parabolic, and exponential gap functions, respectively.

Author(s)	Method	P (kbar)	Function	A (eV)	β (1/kbar)	B (eV)	$E_g(0)$ (eV)	$(\partial E_g/\partial P)_{P=0}$ (10^{-2} eV/kbar)	$(\partial^2 E_g/\partial P^2)_{P=0}$ (10^{-4} eV/kbar^2)
Long[a]	Conductivity and Hall coefficient	0–2	Lin.				0.336	−1.60	
Neuringer[b]	Infrared absorption	0–1.1	Lin.					$-1.8 \pm 0.3 \vec{E} \| \vec{c}$ $-2.2 \pm 0.4 \vec{E} \perp \vec{c}$	
Becker *et al.*[c]	Conductivity	0–6	Lin.				0.33	−1.3	
Koma *et al.*[d]	Conductivity and Hall coefficient	0–7	Par.					−1.47	5.46
Blum and Deaton[e]	Electrical resistance	0–43	Exp.	0.3897	0.04362	0.05973	0.33	−1.7	7.42
Anzin *et al.*[f]	Transmission	0–6.7	Exp.	0.3229 ± 0.0001	0.0630 ± 0.0001	0	0.3229 ± 0.0001	-2.034 ± 0.004	12.82
Anzin *et al.*[f]	Photoconductivity	0–6.2	Exp.	0.3296 ± 0.0009	0.061 ± 0.001	0	0.3296 ± 0.0009	-2.01 ± 0.04	12.26
Pine *et al.*[g]	Laser emission	0–8	Par.	(0.3335)	(0.0591)	(0)	0.3335 ± 0.0005	-2.0 ± 0.05	10.4 ± 0.4
Starkloff and Joannopoulos[h]	SCPP $\alpha = 1$	0, 8, 38	Par.				0.44	−1.524	3.728
Isomäki *et al.*[i]	SCSOPW $\alpha = 1$	0, 8, 38	Exp.	0.3539	0.05273	0.1132	0.24	−1.866	9.838
	SCSOPW $\alpha = \frac{2}{3}$	0, 8, 38	Exp.	0.3346	0.05318	0.2972	0.04	−1.779	9.462

[a]Reference 53. [b]Reference 54. [c]Reference 55. [d]Reference 56. [e]Reference 36. [f]Reference 57. [g]Reference 30. [h]References 21 and 22. [i]This work.

and the SCPP results support this conclusion, because the VB maximum and the CB minimum occur at the same point H. [The distances to the next VB maximum at M and to the next CB minimum at A are 0.1–0.3 eV (Table I).]

Pine *et al.*[30] suggest that the minimum direct gap at H should shift to A with increasing pressure when Te approaches the metallic phase. To support this argument they have performed empirical pseudopotential calculations resulting in an indirect optical gap $H \rightarrow A$. This indirect gap should then precede the final shift into a direct gap at A. However, both the SCSOPW and the SCPP results are in disagreement with this suggestion because the distance between the CB minimum at H and that at A continually increases with increasing pressure (Table I). [The distance between the VB maximum at A and that at H of ≈ 1 eV decreases slightly (≈ 0.1 eV up to 38 kbar).]

All experimental gap values at zero pressure are about 0.33 eV (Table II). If the relativistic correction of −0.13 eV from the relativistic Korringa-Kohn-Rostoker (KKR) calculations[12] are taken into account the SCPP gap of 0.44 eV (Table I) becomes 0.31 eV which is very near the experimental value. However, in general the nonrelativistic X_α gap is known to underestimate the experimental gap especially for smaller values of α. Therefore, we consider the values 0.24 and 0.04 eV of our SCSOPW gaps for the α values 1 and $\frac{2}{3}$, respectively, to be close to the values the X_α theory should give. The relativistic corrections would diminish these gaps further. However, it is obvious both from Fig. 5, where some gap functions are displayed, and Table II, that the form of the SCSOPW gap function (i.e., coefficients A and β in

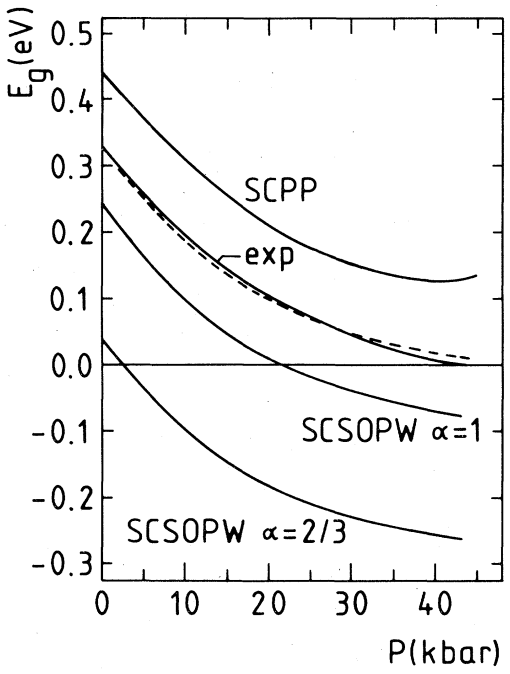

FIG. 5. The behavior of the optical gaps E_g under the hydrostatic pressure P. SCSOPW $\alpha = 1$ and $\frac{2}{3}$ denote the exponential SCSOPW gap functions with the coefficients from Table II. SCPP denotes the parabolic SCPP gap function (Ref. 21) (Table II). exp denotes the exponential gap function fitted to the experiments of Blum and Deaton (Ref. 36) (Table II). The dashed line is the theoretical SCSOPW estimate described in the text.

TABLE III. The SCSOPW core levels of Te. The distances between the core levels and the VB maximum are given in eV.

Level	$\alpha=\frac{2}{3}$ 0 kbar	$\alpha=1$ 0 kbar	Rel. corr. $\alpha=1$ 0 kbar	Exp.[a]	Exp.[b]	$\alpha=\frac{2}{3}$ 8 kbar	$\alpha=1$ 8 kbar	$\alpha=\frac{2}{3}$ 38 kbar	$\alpha=1$ 38 kbar
1*s*	30337.2	30558.7	32032.7			30337.4	30559.1	30337.8	30559.4
2*s*	4533.1	4601.1	4929.4			4533.3	4601.3	4533.7	4601.7
2*p*	4258.5	4332.6	4648.4			4258.7	4332.8	4259.2	4333.1
			4393.6						
3*s*	897.3	922.4	1000.5		1004.9	897.5	922.6	897.9	922.9
3*p*	781.2	807.1	875.1		870.6	781.4	807.2	781.8	807.6
			827.5		819.8				
3*d*	564.2	590.2	606.4		583.3	564.5	590.4	564.9	590.7
			595.2		573.0				
4*s*	147.8	156.0	172.3		169.5	148.0	156.2	148.4	156.5
4*p*	107.8	115.5	129.1			108.0	115.7	108.4	116.0
			119.9						
4*d*	40.1	46.1	48.7	41.8	42.0	40.3	46.3	40.7	46.6
			47.1	40.3	40.5				

[a]From Ref. 49.

[b]From Ref. 50.

Table II) is very insensitive to the changes of α whereas the vertical position of the function (i.e., coefficient B in Table II) is sensitively affected by the value of α. To give a theoretical estimate about the possible closing of the gap we have shifted the SCSOPW $\alpha=1$ gap function vertically upwards to start at the experimental value 0.33 eV (dashed curve in Fig. 5). Our theoretical estimate at 40 kbar is 0.019 eV, which is less than kT at room temperature. Thus, we may theoretically expect trigonal Te to become conducting at $\approx$40 kbar which is about the same as the experimental semiconductor-metal transition pressures of 38–44 kbar.[31,33–37] The parabolic SCPP gap function when shifted to start at the experimental gap value would attain its minimum value of 0.019 eV at 41 kbar very close to the SCSOPW value.

The distances between the core levels and the VB maximum at different pressures P are given in Table III for the α values $\frac{2}{3}$ and 1. We give in the fourth column the distances for the relativistically corrected (see Ref. 46) core levels ($\alpha=1$, $P=0$ kbar) and in the fifth and sixth columns the corresponding experimental core levels of Pollak *et al.*[49] and Shevchik *et al.*[50] One immediately notices that the effect of hydrostatic pressure is almost negligible. The distances of all SCSOPW core levels increase with increasing pressure at the same rate and this increase at 38 kbar is only 0.5–0.6 eV. The fourth column in Table III does not include the relativistic corrections at the VB maximum which will reduce the given values slightly (according to Ref. 12 $\approx$0.4 eV). The relativistically corrected SCSOPW levels (except the 3s level) are more negative than the corresponding experimental values. This result is in accordance with the fact that the relaxation corrections are expected to be positive.[62,63] Only the 3s level is slightly too positive.

IV. CONCLUSIONS

We have presented our theoretical self-consistent band structures and core-level spectra for Te under applied hydrostatic pressure with α values $\frac{2}{3}$ and 1. Disregarding some details, we find that our SCSOPW ($\alpha=1$) bands agree quantitatively well with the SCPP ones. We find a direct optical gap at the corner point H of 0.24 and 0.04 eV for the α values 1 and $\frac{2}{3}$, respectively. Five peaks of our $\alpha=1$ VDOS are in good quantitative agreement with the XPS ones. The optical gap remains at H at all pressures, and the distances to the next VB maximum at M and CB minimum at A increase with increasing pressure. At room temperature the SCSOPW gap becomes less than kT at $\approx$40 kbar which approximately coincides with the experimental semiconductor-metal transition pressures. The core levels are found to be very insensitive to hydrostatic pressure. The relativistically corrected $\alpha=1$ levels are more negative than the experimental ones (except 3s), thus allowing positive relaxation corrections.

ACKNOWLEDGMENTS

Two of us (H.I. and J.v.B.) wish to express their gratitude to Professor M. A. Ranta for his continuous support. A significant part of the present work was carried out by the above authors in the Electron Physics Laboratory of Helsinki University of Technology. We wish to thank the Swedish Academy of Technical Sciences in Finland for financial support in connection with the publication. We also want to thank the computer centers of Helsinki University of Technology and NORDITA for the pleasant cooperation.

---

*Present address: Helsinki University of Technology, SF-02150 Espoo 15, Finland.

†Currently at Cornell University, School of Electrical Engineering, Ithaca, New York 14853.

[1] *The Physics of Selenium and Tellerium*, edited by E. Gerlach and P. Grosse (Springer, Berlin, 1979), Vol. 13.

[2] O. Madelung and J. Treusch, in *The Physics of Se and Te*, edited by W. C. Cooper (Pergamon, Oxford, 1969).

[3] P. Grosse, in *Springer Tracts in Modern Physics*, edited by G. Hohler (Springer-Verlag, Berlin, 1969), Vol. 48.

[4] J. D. Joannopoulos in Ref. 1.

[5] J. R. Reitz, Phys. Rev. 105, 1233 (1957).

[6] R. Sandrock and J. Treusch, Solid State Commun. 3, 361 (1965).

[7] R. E. Beissner, Phys. Rev. 145, 479 (1966).

[8] M. Hulin, J. Phys. Chem. Solids 27, 441 (1966).

[9] J. Treusch and R. Sandrock, Phys. Status Solidi 16, 487 (1966).

[10] M. Picard and M. Hulin, Phys. Status Solidi 23, 563 (1967).

[11] H.-G. Junginger, Solid State Commun. 5, 509 (1967).

[12] B. Kramer and P. Thomas, Phys. Status Solidi 26, 151 (1968).

[13] M. Hulin and M. Picard, Solid State Commun. 7, 1587 (1969).

[14] K. Maschke, Phys. Status Solidi 47, 511 (1971).

[15] M. Schlüter, Int. J. Quantum Chem. S 7, 527 (1973).

[16] W. E. Rudge, C. D. Chekroun, and I. B. Ortenburger, Bull. Am. Phys. Soc. 18, 350 (1973).

[17] B. Kramer, K. Maschke, and L. D. Laude, Phys. Rev. B 8, 5781 (1973).

[18] M. Schlüter, J. D. Joannopoulos, and M. L. Cohen, Phys. Rev. Lett. 33, 89 (1974).

[19] J. D. Joannopoulos, M. Schlüter, and M. L. Cohen, Phys. Rev. B 11, 2186 (1975).

[20] D. W. Bullett, Philos. Mag. 32, 1063 (1975).

[21]T. Starkloff and J. D. Joannopoulos, J. Chem. Phys. 68, 579 (1978).
[22]T. Starkloff and J. D. Joannopoulos, Phys. Rev. B 19, 1077 (1979).
[23]Some preliminary results were published earlier. J. v. Boehm, H. Isomäki, P. Krusius, and T. Stubb in Ref. 1.
[24]J. von Boehm and P. Krusius, Int. J. Quantum Chem. 8, 395 (1974).
[25]P. Krusius, J. von Boehm, and T. Stubb, Phys. Status Solidi B 67, 551 (1975).
[26]B. Moreth, Phys. Rev. Lett. 42, 264 (1979).
[27]M. Kastner and R. R. Forberg, Phys. Rev. Lett. 36, 740 (1976).
[28]H. Wendel, R. M. Martin, and D. J. Chadi, Phys. Rev. Lett. 38, 656 (1977).
[29]J. D. Joannopoulos, T. Starkloff, and M. Kastner, Phys. Rev. Lett. 38, 660 (1977).
[30]A. S. Pine, N. Menyuk, and G. Dresselhaus, Solid State Commun. 31, 187 (1979).
[31]P. W. Bridgman, Proc. Am. Acad. Arts Sci. 74, 425 (1942).
[32]P. W. Bridgman, Proc. Am. Acad. Arts Sci. 81, 169 (1952).
[33]G. C. Kennedy and P. N. La Mori, J. Geophys. Res. 67, 851 (1962).
[34]S. S. Kabalkina, L. F. Vereshchagin, and B. M. Shulenin, Zh. Eksp. Teor. Fiz. 45, 2073 (1963) [Sov. Phys. JETP 18, 1422 (1964)].
[35]J. C. Jamieson and D. B. McWhan, J. Chem. Phys. 43, 1149 (1965).
[36]F. A. Blum and B. C. Deaton, Phys. Rev. 137, A1410 (1965).
[37]G. C. Vezzoli, Z. Kristallogr. 134, 305 (1971).
[38]G. Doerre and J. D. Joannopoulos, Phys. Rev. Lett. 43, 1040 (1979).
[39]P. Krusius, T. Stubb, H. Isomäki, and J. v. Boehm, Phys. Rev. B 22, 2955 (1980) (following paper).
[40]P. A. M. Dirac, Proc. Cambridge Philos. Soc. 26, 376 (1930).
[41]R. Gáspár, Acta Phys. Acad. Sci. Hung. 3, 263 (1954).
[42]W. Kohn and L. J. Sham, Phys. Rev. 140, A1133 (1965).
[43]J. C. Slater, Phys. Rev. 81, 385 (1951).
[44]J. C. Slater, in *Advances in Quantum Chemistry*, edited by P.-O. Löwdin (Academic, New York, 1971), Vol. 6, p. 1.
[45]In fact the present calculations were started at this point by using the self-consistent valence electron density of Se as the starting point.
[46]F. Herman and S. Skillman, *Atomic Structure Calculations* (Prentice-Hall, Englewood Cliffs, 1963).
[47]P. Unger and P. Cherin, in Ref. 2, p. 223.
[48]R. Keller, W. B. Holzapfel, and H. Schulz, in Refs. 21 and 22.
[49]R. A. Pollak, S. Kowalczyk, L. Ley, and D. A. Shirley, Phys. Rev. Lett. 29, 274 (1972).
[50]N. J. Shevchik, M. Cardona, and J. Tejeda, Phys. Rev. B 8, 2833 (1973).
[51]M. Schlüter, J. D. Joannopoulos, M. L. Cohen, L. Ley, S. P. Kowalczyk, R. A. Pollak, and D. A. Shirley, Solid State Commun. 15, 1007 (1974).
[52]M. Wautelet and L. D. Laude, Phys. Rev. Lett. 38, 40 (1977).
[53]D. Long, Phys. Rev. 101, 1256 (1956).
[54]L. J. Neuringer, Phys. Rev. 113, 1495 (1959).
[55]W. Becker, W. Fuhs, and J. Stuke, Phys. Status Solidi B 44, 147 (1971).
[56]A. Koma, T. Tani, and S. Tanaka, Phys. Status Solidi B 66, 669 (1974).
[57]V. B. Anzin, M. I. Eremets, Y. V. Kosichkin, A. I. Nadezhdinskii, and A. M. Shirokov, Phys. Status Solidi A 42, 385 (1977).
[58]Y. V. Kosichkin, in Ref. 1.
[59]S. Tutihasi, G. G. Roberts, R. C. Keezer, and R. E. Drews, Phys. Rev. 177, 1143 (1969).
[60]P. Grosse and K. Winzer, Phys. Status Solidi 26, 139 (1968).
[61]H. Shinno, R. Yoshizaki, S. Tanaka, T. Doi, and H. Kamimura, J. Phys. Soc. Jpn. 35, 525 (1973).
[62]O. Goscinski, B. T. Pickup, and G. Purvis, Chem. Phys. Lett. 22, 167 (1973).
[63]O. Goscinski and A. Palma, Chem. Phys. Lett. 47, 322 (1977).